Welding Research

Sponsored by the Welding Research Council of the Engineering Foundation

WRC

SUPPLEMENT TO THE WELDING JOURNAL, JUNE 1970

Fatigue Tests on a Welded Beam with Pre-Existing Cracks

The relationship between crack lengths in the flange and web are studied using a fracture mechanics model for a three-ended crack, and results are correlated with observed crack growth

BY P. J. MAREK, M. PERLMAN, A. W. PENSE, AND L. TALL

ABSTRACT. This paper presents the results and discussion of an experimental investigation of a welded beam with a pre-existing three-ended crack in the last phase of its fatigue life.

The stress and strain redistribution was recorded and compared with the results obtained from a mathematical model. The variation of strain range and mean strain in front of the crack was analyzed considering a typical residual stress pattern, actual mechanical properties of A514J steel and a three-ended crack in the beam subjected to cyclic loading. Reasonable correlation between measured and theoretical results was observed.

The relationship between crack lengths in the flange and in the web was studied using a fracture mechanics model for a three-ended crack in a beam and results were correlated with the crack growth observed.

The fracture surface study reveals a transition from smooth to rough texture as the crack grows from initial size to final beam failure.

The microstructure of A514J steel is sufficiently fine that the direction of fracture is determined by the applied stress. On the microscopic level, however, the fracture path follows inclusions, carbides and microstructure boundaries. A delamination tendency increases during the final stage of fracture growth.

P. J. MAREK, M. PERLMAN, A. W. PENSE and L. TALL are with Lehigh University, Bethlehem, Pa.

Paper presented at the AWS 51st Annual Meeting held in Cleveland, Ohio, during June 8-12, 1970.

Introduction

As part of a larger study of the low-cycle fatigue of joined structures, a pilot program was undertaken to investigate the fatigue behavior of a wide flange welded beam with a three-ended crack. The initial crack was formed during high-cycle testing of the beam (Phase A). A second loading schedule was instituted in this program to continue the crack growth during the tests reported here (Phase B). Both strain redistribution and crack propagation were recorded as the crack extended under constant external loading conditions and the remaining net section was subjected to increasing severity of stress and strain.

The tests conducted were designed:

1. To obtain pilot information about propagation of the three-ended crack.

2. To record and study the redistribution of stress and strain in the flange and web.

3. To study the interaction of the crack propagation in the flange and web considering applied cyclic loading, material properties and residual stresses in the beam.

4. To correlate recorded strain redistribution with the results of a theoretical analysis using a mathematical model.

5. To try different kinds of measurements for low-cycle fatigue testing on beams.

The test was not typical of normal fatigue testing procedures, since the beam tested in this study had already been tested with Phase A loading until a crack formed and was detected. The loading conditions in Phase A were different from those in this program. The beam had certain advantages with respect to the purpose of this study—that is, to obtain information about stress and strain observations under significant plastic yielding conditions. They were:

1. The crack initiation had already occurred and crack propagation thus could be readily observed and monitored.

2. Comparisons of changing crack growth morphology could be made in one specimen.

3. The presence of a pre-existing complex crack shape (three-ends) presented an interesting experimental and analytical problem for study.

4. The beam was fabricated by welding, allowing an analysis of the influence of welding on its fatigue behavior.

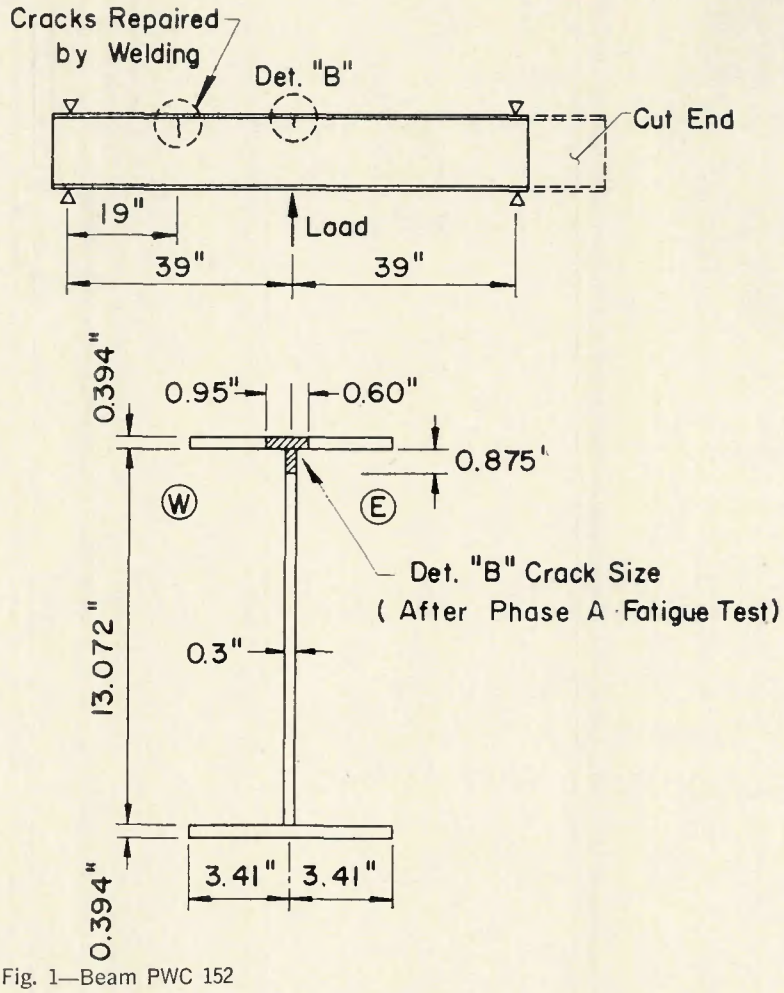

Fig. 1—Beam PWC 152

Description of Test

Specimen

The wide flange beam tested was fabricated by welding from oxygen-cut plates of A514 steel—Fig. 1. This beam was tested under Phase A high-cycle fatigue conditions where the stress range in the flanges was 42 ksi and the maximum nominal stress was +32 ksi.[1]

After 397,000 cycles of such loading, the crack shown as detail B in Figs. 1 and 2 was obtained under one of the load application points (four point loading). Cracks not to be investigated in this program were repaired and the beam was cut to length and positioned as shown in Fig. 1 for the second phase of the fatigue test (Phase B).

Instrumentation

Crack propagation, strains and deflections were measured and recorded during the fatigue test. The following instrumentation was used in the testing:

1. Strain gages (marked 1, 2, 10, 20, 3, 4, 5 in Figs. 2 and 3).

2. The static strains were recorded using a digital strain indicator and the cyclic strains were recorded using a recorder and an oscilloscope.

3. Crack propagation gages (marked a, b, c, d) in Fig. 2. The propagation was recorded by a strip chart recorder.

4. A microscope was used for visual crack propagation readings.

5. A dial gage was used for measuring deflection of the beam.

Test Program and Recordings

The Phase B fatigue test consisted of loading the beam with a central crack (Fig. 1) and monitoring crack growth as the original crack extended across the flange and down through the web. The test ended when one side of the tension flange marked *W* in Fig. 1 was completely severed.

The loading of the beam in this fatigue test was started by loading statically in increments to the maximum load of 80 kips while all recording channels were checked. The first set of strain gage readings were taken for different loads as the maximum load was applied. Vertical deflection for maximum load was recorded.

The dynamic test consisted of loading between the range of 80 and 30 kips. This resulted in a maximum nominal stress of +36.2 ksi and a stress range of 22.6 ksi in the flanges. The testing machine was operated at 250 cycles/min to apply 5000 cycles of alternating load between measurements. The maximum dynamic load was adjusted slightly to obtain the same deflection as was recorded for static load.

After each 5000 load cycles the strains were recorded under static loads of 80 kips and 0 kips. Static readings for 15000 and 20000 cycles are missing due to changes in recorder instrumentation.

Satisfactory visual recording of crack growth rate was obtained by using the microscope; however, there were some difficulties in following the crack tip at the beginning of the test when the crack was short. Even under an 80 kip static load the crack was not open enough to make the tip position completely clear. Later in the test it was possible to follow the crack tip while cycling with good accuracy.

Crack opening was measured for maximum and minimum static load for the last 5000 cycles of load.

Metallographic Examination

At the conclusion of the Phase B test, sections of the failed beam were made available for metallographic examination. The tension flange and adjacent web were sectioned as shown on Fig. 4. All sectioning was done by saw cutting with lubricant to avoid any heat affects due to the sectioning procedure. These specimens were polished by standard metallographic procedures and were examined and photographed before and after etching.

Test Results

Crack Propagation and Strain Recording

After comparison of visual records with records from crack propagation gages, the shape of the crack (Fig. 2) and the relationship between the number of cycles and crack length (Fig. 5) were obtained. For the flange half marked *W*, Fig. 5 shows the information available about the crack propagation on both the top and bottom surfaces separately and also an average value curve. In the range from zero to 37,000 cycles the crack propagation rate was almost constant, then it increased gradually to a very high value before failure—Figs. 6 and 7.

The strain gage readings are plotted in Figs. 8-10. The top curves correspond to strain due to static loads of 80 kips, and the bottom curves are assumed to correspond with the gradually developed and/or redistributed residual stress at 0 kips load.

The recording of crack propagation in the web was not satisfactory, and

only fragmentary information was obtained. It includes the initial crack length, the final crack length and the number of cycles accumulated when the crack tip reached strain gage no. 3. The assumed crack propagation is shown in Fig. 5. The final crack length includes an increment, Δcr, probably caused by impact when the flange failed.

Metallographic Results

The fracture surfaces were examined macroscopically to characterize the nature (rough, delaminated, smooth) and orientation of the fracture to the test beam—Fig. 4. After sectioning and polishing, the specimens were examined as polished and after a Nital etch.

Figure 11 is a section normal to the flange crack in a region of the crack formed during Phase A testing. Figure 12 is a section normal to the flange crack formed during constant crack propagation in Phase B.

Examination of the fracture surface revealed that the crack started at a tack weld end (Fig. 13) during Phase A. From this point it grew slowly through the flange-to-web weld, the central part of the flange and the top of the web—Fig. 6. This crack was first observed after 386,300 cycles. The tack weld end which caused the crack was not fused to the web and flange (cold lap). The fillet weld subsequently deposited did not melt through this tack weld—Fig. 13.

Discussion

Stress and Strain Redistribution During Testing

To allow theoretical analysis of redistribution of strain and stress in the tested beam, information about residual stress patterns was required. Similar welded shapes had been investigated by sectioning[2, 3] to measure the magnitude of residual stresses developed during fabrication of the beam. The residual stress pattern shown in Fig. 14 was obtained for a similar beam, of the same heat and fabrication procedure as the beam tested. The average of stresses at corresponding points on both surfaces was considered representative and, for the theoretical analysis, was further adjusted to obtain symmetrical distribution with respect to both axes.

The stress distribution in the flange and the web was first analyzed theoretically using the simplified mathematical model using "lumped volumes" and computer programs developed for a plate with a crack[4] and for a three-ended crack in a beam.[5] The average residual stresses and actual mechanical properties of this beam and steel

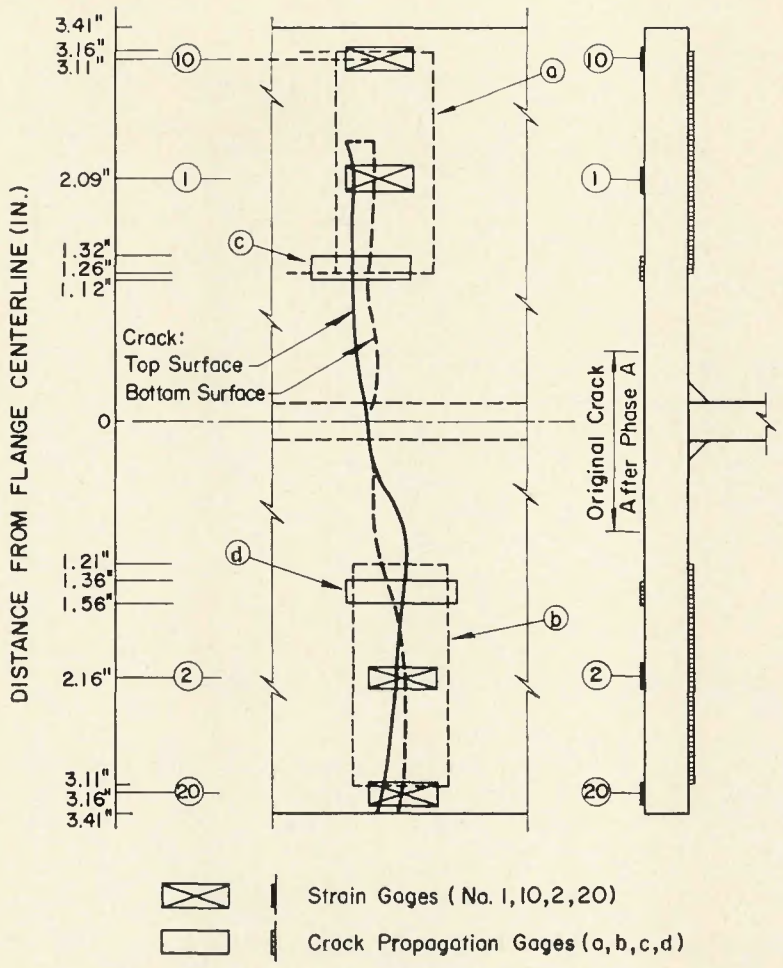

Fig. 2—Shape of the crack and the position of strain gages in the flange

were considered.

The theoretical stress distributions for loading (P=80 kips) for different crack sizes are plotted in Fig. 15 for a

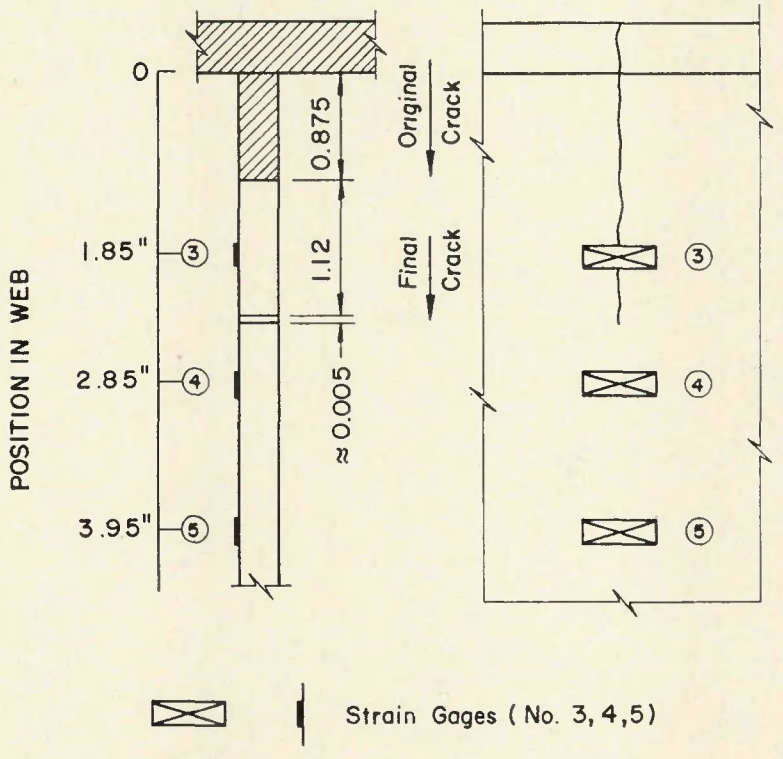

Fig. 3—Crack in the web and position of the strain gages

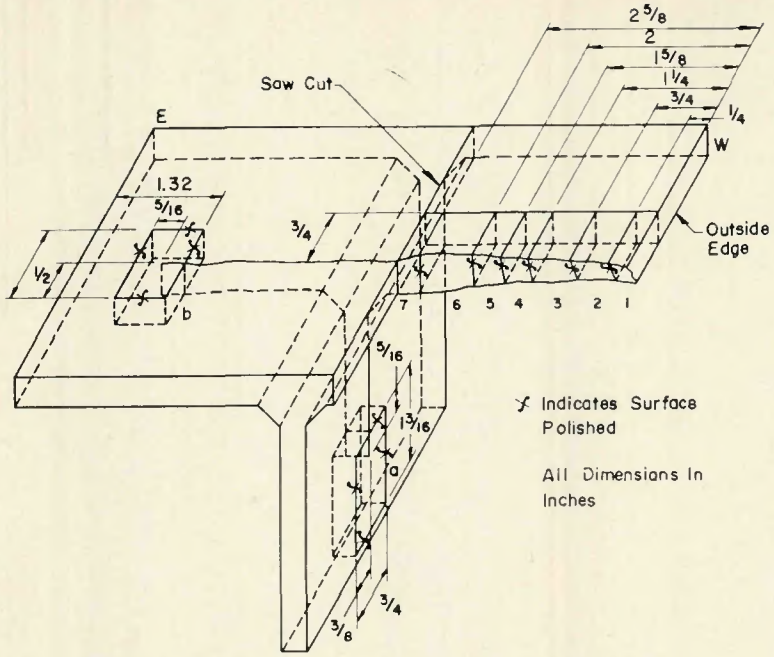

Fig. 4—Sectioning of the beam for metallurgical investigation

flange-web three-ended crack. The distribution curve corresponding to the initial crack size was used as a reference line to plot stresses evaluated from strains recorded in the test. The comparison of the theoretical and recorded data may be considered satisfactory.

Using the mathematical model for a beam with a three ended crack, the variation of maximum and minimum strain in front of the crack was evaluated and plotted in Fig. 16. The strains which are shown cannot be considered as wholly accurate because of the simplifying assumptions and the large size of finite elements in the computer program. Nevertheless, the relative variation of strains during significant phases in crack propagation are indicated.

After crack initiation, the strain range and mean strains, both in the flange and web, increase very rapidly due to release of residual tension stress. With continued crack growth the mean strains increase to a maximum in both flange and web. The mean strains thereafter decrease in the flange and web, while the strain range increases at a lower rate. In the last portion of the fatigue life, the mean strain and strain range in the flange increases very rapidly, while in the web the strain range remains nearly constant and the mean strain continues to decrease.

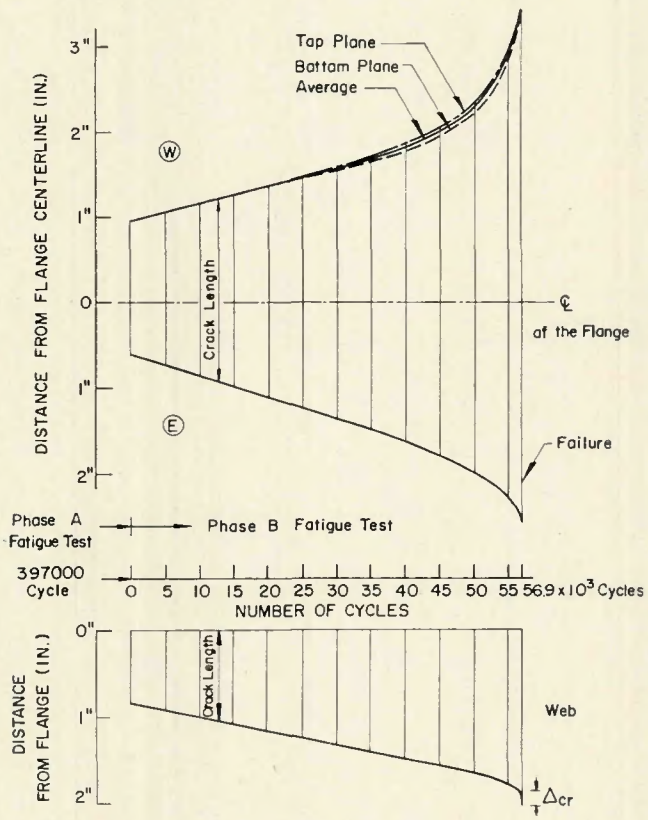

Fig. 5—Crack length vs. number of cycles

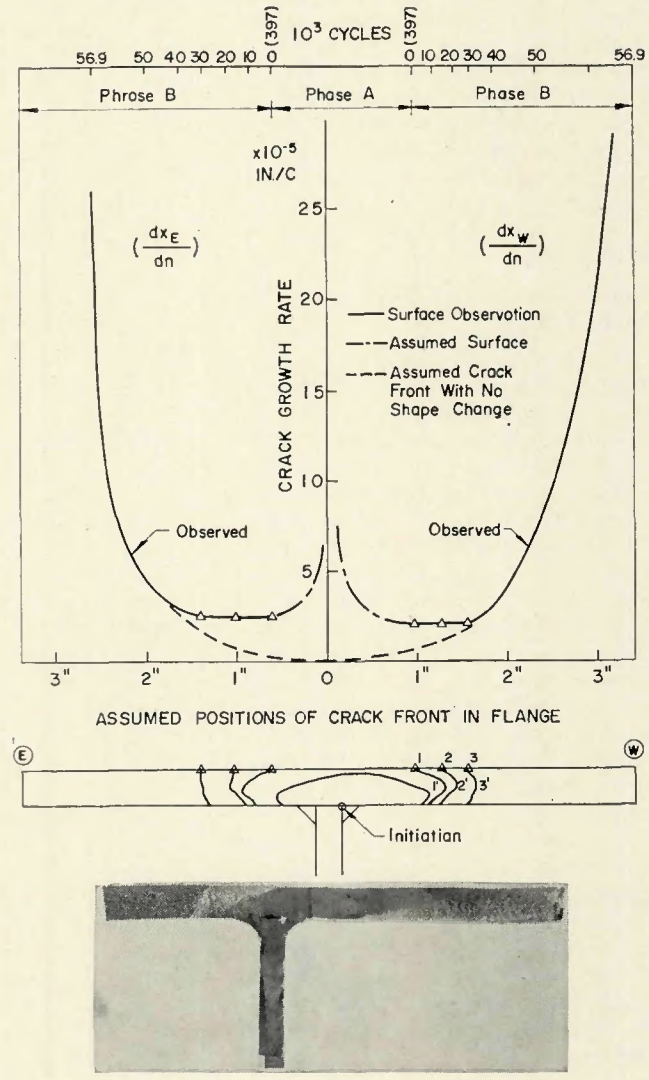

Fig. 6 (right)—Crack growth rate vs. position in the flange

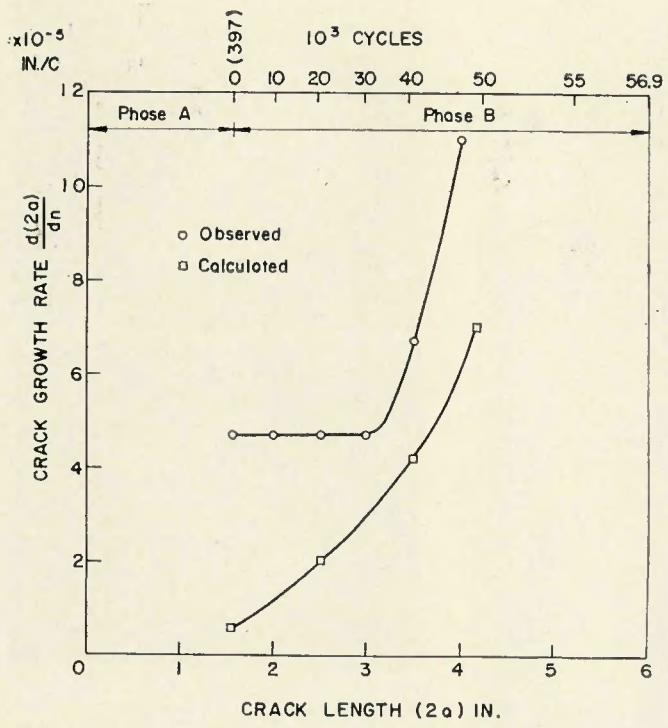

Fig. 7—Crack growth rate vs. crack length (average)

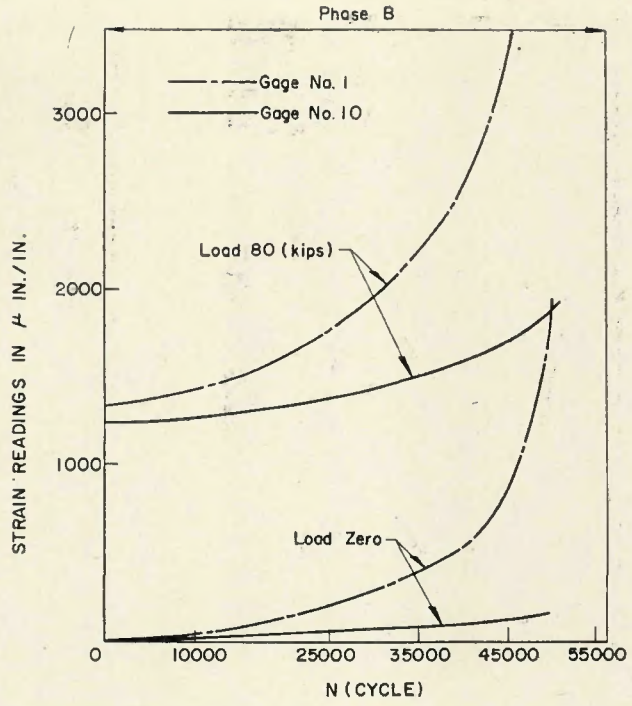

Fig. 8—Strain readings (gages 1, 10)

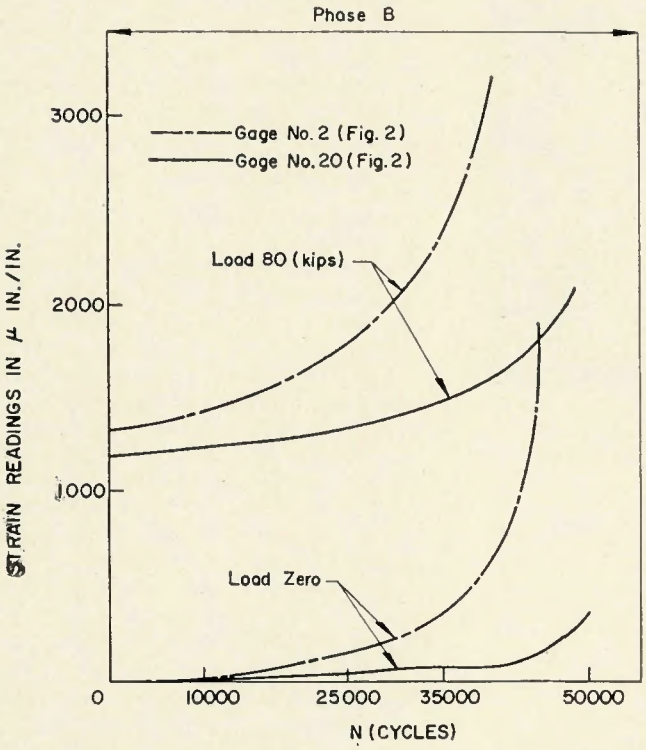

Fig. 9—Strain readings (gages 2, 20)

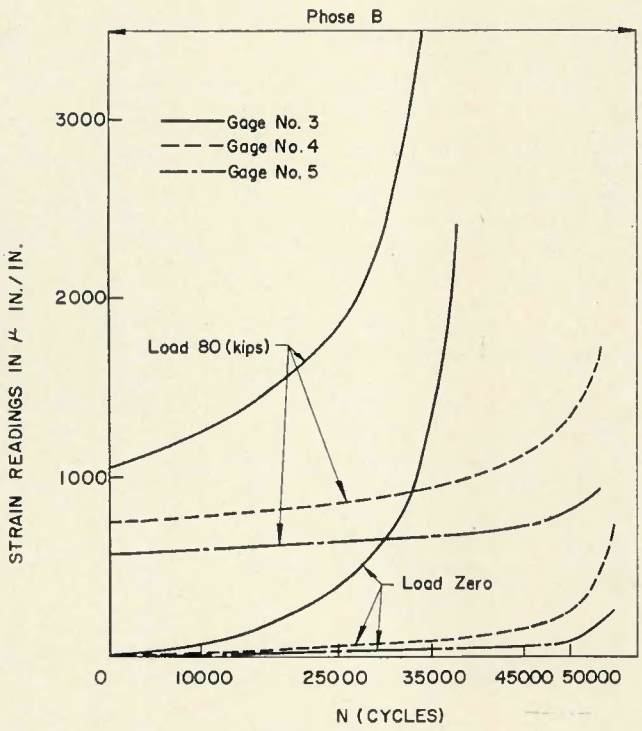

Fig. 10—Strain readings (gages 3, 4, 5)

This strain history relates fairly well to observed crack growth in this test. The three-ended crack grew in a coupled manner between web and flange during the early portions of the Phase B testing—Figs. 5, 6, 7 and 16. Late in Phase B the flange crack grew at an accelerating rate to final failure, while no appreciable web crack growth was observed.

Crack Propagation

As mentioned above, the three-ended crack formed in Phase A testing grew as shown in Figs. 5–7. Starting from the unfused tack weld the crack grew through the web and flange —Fig. 6. When the initial crack first broke through to the outside surface of the beam tension flange, it grew very rapidly on the surface since only a thin ligament was left intact due to the overall shape of the fracture. This is shown in Fig. 6 as the assumed surface crack growth rate during Phase A.

It is important to note at this point that observations during testing are limited to those increments of fracture which are detected on the surface of the beam. In this program such data were collected visually and with gages. These observations can be somewhat

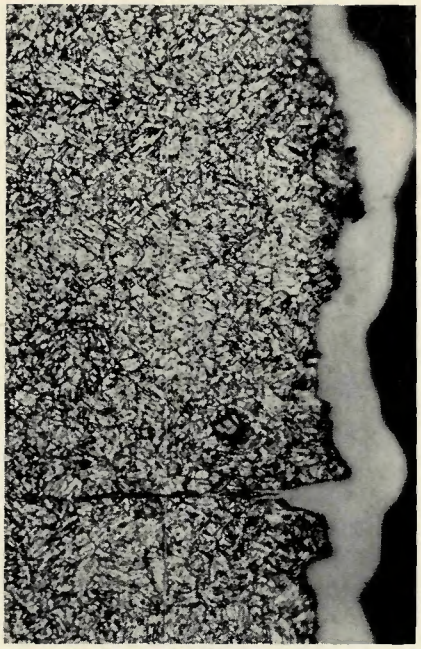

Fig. 11—Section normal to fracture surface, Phase A testing, specimen 7. Nital etch. X250 (reduced 25% on reproduction)

misleading with respect to the complete fracture process.

The observed data plotted on Fig. 6 show that crack growth was uniform for nearly 40,000 cycles of testing after which rapid crack propagation to final failure occurred in only 17,000 additional cycles. As indicated in Fig. 6, the observed readings need not be representative of the true fracture behavior. The crack front shape changed as the test progressed. During this period equal increments indicated as 1″-2″ and 2″-3″ were observed on the surface while the crack center was probably moving with increasing increments shown as 1″-2″ and 2″-3″. At the third position, the stable crack front shape could have been reached and crack propagation would then continue by translation under conditions of increasing loading severity.

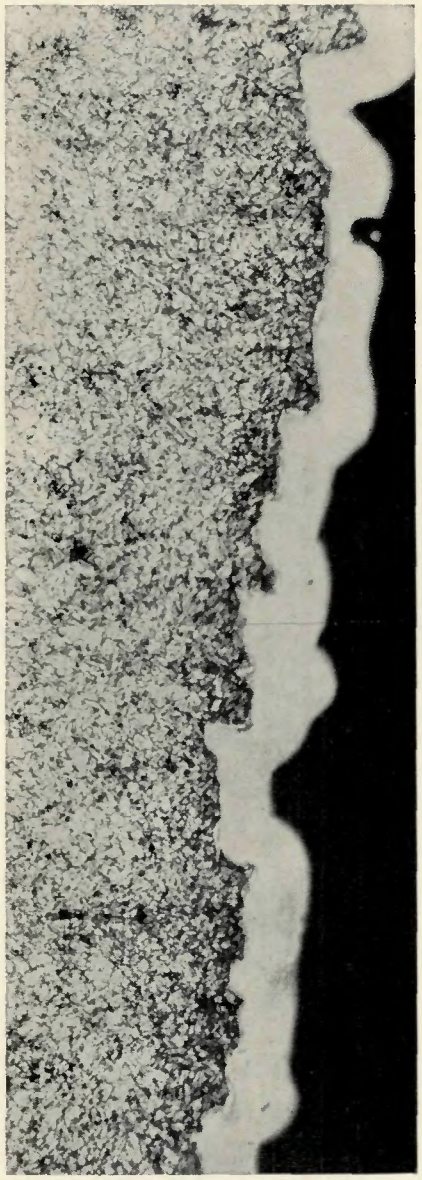

Fig. 12—Section normal to fracture surface, Phase B testing, specimen 5. Nital etch. X250 (reduced 22% in reproduction)

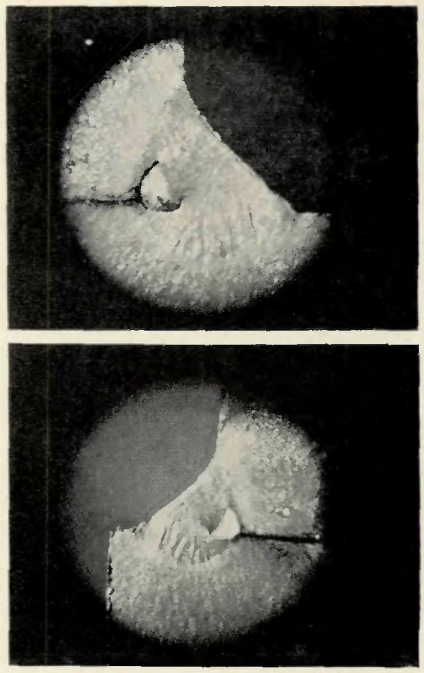

Fig. 13—Web-to-flange fillet welds in fracture surface

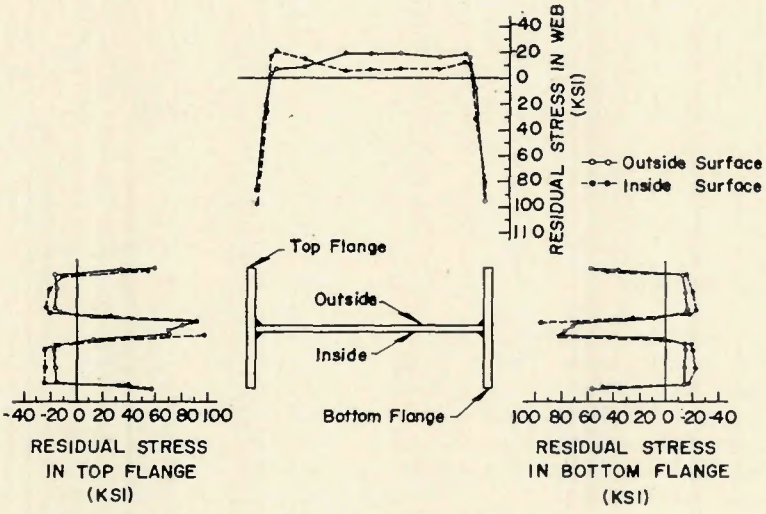

Fig. 14—Residual stress distribution in the beam

The point to be drawn from Fig. 6 is that observed results may not reveal the true crack growth rate. Examination after final fracture is necessary to understand more fully the crack propagation.

Influence of the Three Ended Crack

As a result of Phase A testing, the beam tested had an initial three-ended crack—Figs. 1, 2, 3 and 6. In further testing the crack in the flange and web grew in an interrelated manner as schematically indicated on Fig. 17.

Using a three-ended crack analysis based on a fracture mechanics approach,[6] Table 1 was computed considering the Phase B loading and stress redistribution, the material properties of ASTM A514 steel and the observed crack lengths. For each position of the crack, the ΔK in the flange and web are indicated. The outlined boxes correspond to crack length values observed. A review of the values tabulated shows that the three-ended crack extends apparently by following a path which maximizes the total ΔK in flange and web (any adjacent box has a lower ΔK total). This is equivalent to saying that the crack grew by maximizing the release of stored energy in the fracture process.

With the values computed for the flange ΔK. crack growth rates were obtained from tests of plate specimens of the tested steel.[7] These values are plotted in Fig. 7 as the calculated curve. It should be noted that the expected crack growth rate is based on a stable crack front shape, whereas

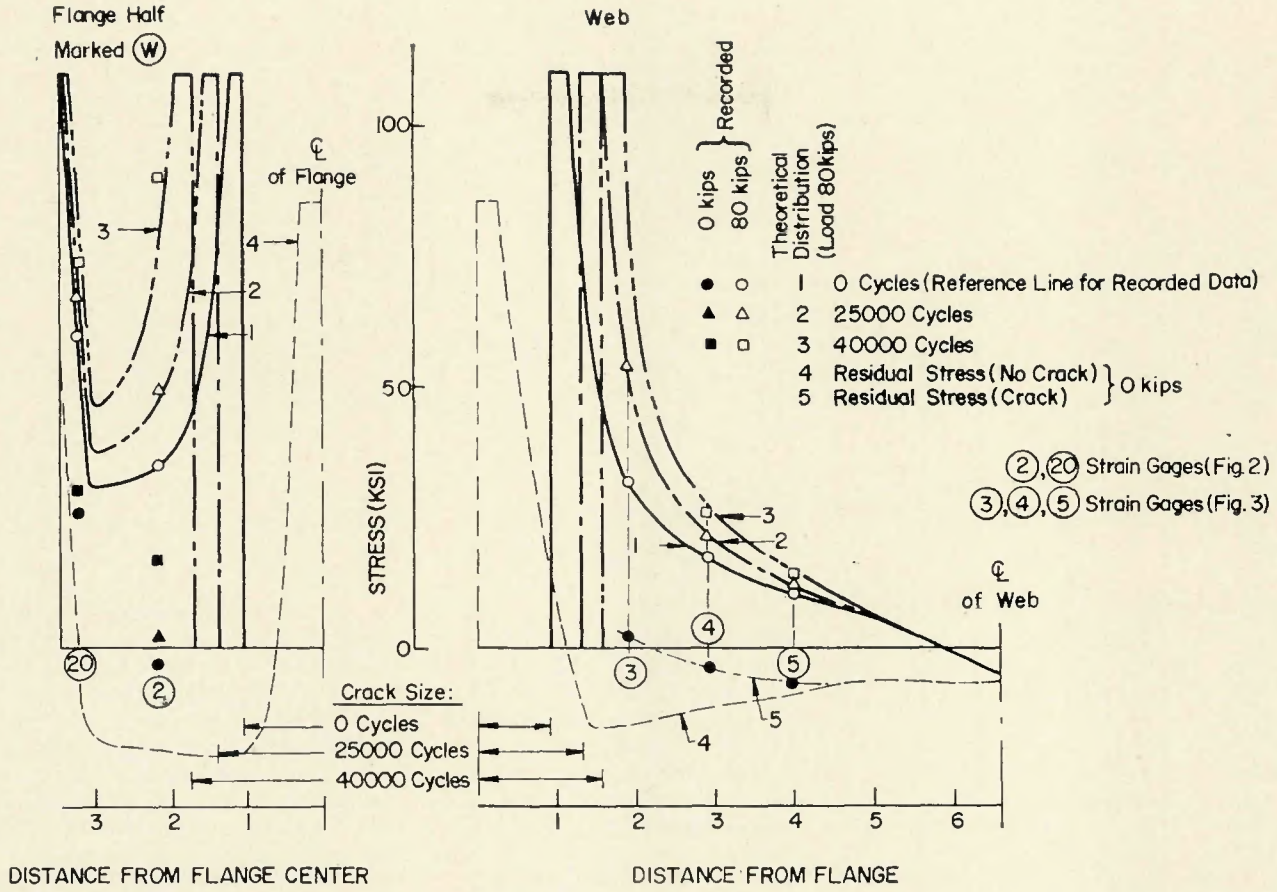

Fig. 15—Stress redistribution in the beam with crack

in the early steps of Phase B testing the observed crack growth rates were influenced by a change in crack shape.

Later in the test, the observed values and those computed follow a similar trend. The analysis assumed a central flange crack which was not the situation tested. With an asymmetric flange crack, one end of the crack will reach instability with respect to the edge of the flange at a lower total crack length than predicted by the analysis. This might account for the displacement between the observed and calculated curves in Fig. 7.

The fracture mechanics analysis applied in this study is promising as an approach to behavior of cracked beams as it might allow prediction of the relationship of flange crack length vs. the length of web crack as well as fatigue life under complex crack growth conditions.

Metallographic Studies

The beam test was conducted on steel meeting the requirements of ASTM A514, Type J. This is a weldable quenched and tempered steel with a minimum yield strength of 100,000 psi and an ultimate strength of 115,000 to 135,000 psi. The mechanical properties of the plate tested were yield strength 110.23 ksi, tensile strength 118.17 ksi, and elongation, 12.5%.

These properties are attained by heating to not less than 1650° F, water quenching and tempering at not less than 1100° F. Such a heat-treatment usually results in a tempered martensite microstructure.

In the case of A514 Type J, the only special alloying elements added are Mo and B. The necessary hardenability (ability to quench to all martensite) is obtained through a severe cooling rate imposed by roller quenching. Tempering results in a complex and fine tempered martensite structure. This structure may be seen in Figs. 11 and 12.

In the primary hot rolling of plate, inclusions will be elongated in the direction of rolling—that is, parallel to the plate surface. The morphology of these rolled-out inclusions will not be affected by the subsequent quench and tempering operations.

The surface of the Phase A fatigue crack was macroscopically fine textured and was normal to the flange and web—Fig. 6. Microscopic examination of this fatigue crack (Fig. 11) reveals that the crack grows normal to the flange surface independently of any gross microstructural features. There

Table 1—Computational Results Using a Three-Ended Crack Analysis Based on Fracture Mechanics

	ΔK_{flange} / ΔK_{web}	Crack length in flange, in. 1.0	1.55	2.5	3.5	4.35
Crack length in web, in.	0.6	30.9 31.0	36.0 33.4	44.9 37.4		
	0.85	32.6 33.6	37.4 35.7	46.1 39.2	56.2 42.9	
	1.2	34.8 36.7	39.2 38.5	47.7 41.5	57.7 44.6	68.6 47.8
	1.5		40.5 40.4	48.8 43.1	58.9 46.0	69.9 48.8
	1.7			49.6 44.0	59.6 46.7	70.6 49.4

ΔK_{flange} / ΔK_{web} range of stress intensity factor (ksi $\sqrt{in}$)

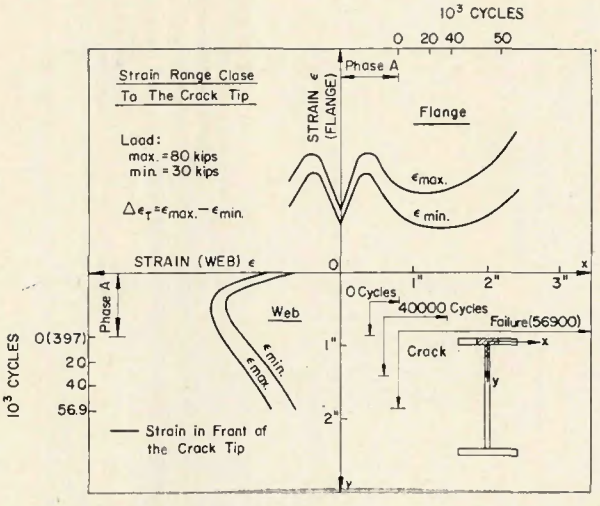

Fig. 16—Variation of the strain-range in front of the crack

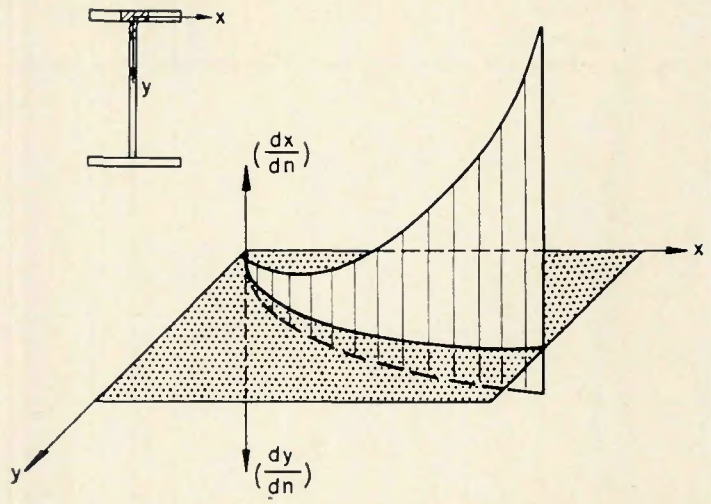

Fig. 17—Schematically indicated crack propagation rates vs. crack length (three-ended crack)

is no strong tendency to delaminate along rolled-out inclusions or to have branched fracture path. The etched section shows that the local fracture path may follow microstructure boundaries, but the overall fracture path seems independent of the microstructural morphology and is responsive mainly to the loading conditions.

A section normal to the crack surface in the region where uniform crack growth was observed is shown in Fig. 12. This section shows that the crack surface follows microstructural boundaries on a fine scale. The overall fracture path is still most responsive to the loading conditions.

At a point 1.6 in. from the edge of the flange, the fracture surface appearance changes from smooth to a more rough texture—Fig. 6. This transition appears to correlate to the point at which a substantial plastic zone at the yield stress level preceeds the growing crack.

At the extremity of the flange the fracture path is inclined to the plane of the flange—Figs. 2 and 4. Delamination along rolled-out inclusions is observed, but this does not deflect the fracture path except in the local region of the inclusions. The fracture surface in this region is fibrous probably due to very high strains occurring prior to fracture.

Conclusion

The purpose of this study was to investigate the fatigue behavior of a welded beam of A514J steel with an initial three-ended crack, in the last phase of its fatigue life, to record crack propagation and stress redistribution. The following conclusions were reached:

1. The crack initiated at the end of a tack weld and grew very slowly through the flange-to-web welds, the central part of the flange, and the top of the web.

2. The variation of range and mean strain in front of the crack tip was analyzed using a mathematical model and computer program considering a typical residual stress pattern and a three-ended crack in the beam subjected to cyclic loading. A reasonable correlation between measured and theoretical strains as well as correlation between strain range and recorded crack propagation rate was observed.

3. The relationship between crack length in the flange and the web was studied and a criterion for crack propagation was developed which correlated with crack growth in the web and flange.

4. The fracture study reveals a transition from smooth to fibrous texture as the crack grows from initial size to final beam failure. This transition is apparently correlated to a very significant stress redistribution and to the increasing size of the yield stress zone at the crack tip. The initial fracture is normal to the applied stress while the final fracture is inclined to the applied stress.

5. The microstructure of A514J steel is sufficiently fine so that its effect on the direction of fracture is minor and the overall fracture path is responsive primarily to loading conditions. On the microscopic level, however, the fracture path follows inclusions, carbides and microstructure boundaries. There is very slight tendency during early fracture propagation to delaminate along rolled-out inclusions. A greater delamination tendency is observed during the final stage of fracture growth.

Acknowledgements

This paper presents the results and discussion of an experimental pilot study of the fatigue of a beam with a crack. The investigation is one phase of a major research program designed to provide information on the behavior and design of joined structure under low-cycle fatigue.

The investigation was conducted at Fritz Engineering Laboratory, the Department of Civil Engineering, and the Department of Metallurgy and Materials Science, Lehigh University, Bethlehem, Pennsylvania. The Office of Naval Research, Department of Defense, sponsored the research under contract N 00014-68-A-514; NR 064-509. The program manager of the overall research project is Lambert Tall.

The guidance of, and the suggestions from, the members of the special Advisory Committee on Low-Cycle Fatigue is gratefully acknowledged. The authors are indebted to Robert D. Stout for his helpful comments.

The authors express their thanks to George R. Irwin for his constructive suggestions during the preparation of the paper and Hiroshi Tada for the computations based on experimental data.

Sincere thanks are due to their coworkers Manfred Hirt and Salvador Lozano for help with the testing and to Kenneth Harpel, Laboratory Superintendent, and his staff, for their assistance during testing. The authors are very grateful to Miss Joanne Mies who typed the paper and to Jack M. Gera and Mrs. Sharon Balogh who prepared the drawings.

Lynn S. Beedle is Director of Fritz Engineering Laboratory; David A. VanHorn is Chairman of the Department of Civil Engineering; George P. Conard II is Chairman of the Department of Metallurgy and Materials Science; and Joseph F. Libsch is Vice-President for Research, Lehigh University.

References

1. Fisher, J. W., Frank, K. H., Hert, M. K., McNamee, B. M.: "Effect of Weldments on the Fatigue Strength of Steel Beams," Fritz Engineering Laboratory Report No. 3342. September 1969.

2. Lozano, S., and Marek, P., "Residual Stress Redistribution in Welded Beams Subjected to Cyclic Bending (Part I)," Fritz Engineering Laboratory Report No. 358.5, Lehigh University, November 1969.

3. Huber, A. W., and Beedle, L. S., "Residual Stress and the Compressive Strength of Steel," WELDING JOURNAL, 33 (12), Research Suppl., 589-s to 614-s, (1954).

4. Smith, R. J., Marek, P., and Yen, B. T., "Stress Distribution in a Plate with a Crack," Fritz Engineering Laboratory Report No. 358.8 (in preparation), Lehigh University.

5. Smith, R. J., Marek, P., and Yen, B. T., "Stress Distribution in a Beam with Crack," Fritz Engineering Laboratory Report No. 358.9. (In Preparation)

6. Irwin, G. R., and Tada, H., "Plasticity Characterization for a Three-Ended Crack," Fritz Engineering Laboratory Report No. 358.11 (in preparation).

7. Nordberg, H., and Hertzberg, R. W., "Fatigue Crack Propagation in A514 Steel," Fritz Engineering Laboratory Report No. 358.7, November 1969.

East European Welding Research News

By Rudolph O. Seitz

EAST GERMANY

ZIS Mitteilungen 11, No. 11 (Nov. 1969).

• Hirschfeld, G.: Study of the relation between welding and weld parameters in semiautomatic CO_2-shielded welding (1869-80).—An attempt has been made to find some simple relationships between the welding parameters and corresponding weld parameters for the purpose of obtaining basic information for the evaluation of experimental data by means of a computer.

• Schellhase, M.: Arc welding stability examined on the basis of a parameter diagram (1881-89).—All the conceivable parameters which affect the static and dynamic stability of the welding arc are arranged and related to each other in the form of block diagrams to show the ramifications of their effect on the arc.

• Heinig, W. and Nitzsche, R.: Theoretical studies toward improving the control action of resistance spotwelding machines (1890-1900).—The growing trend toward automation in spotwelding requires a thorough study of the factors affecting spotweld quality. It is desirable to find a single factor which reflects the process of forming a spotweld with sufficient accuracy so that it can be used to obtain welds of consistent quality. One of these factors examined by the author is the temperature variation at and in the welding spot.

• Schulze, W.: Problems in the magnetoinductive measuring of the weld gap (1902-07).—After describing the principle of an automatic guiding system for welding heads based on magnetic induction the author discusses various types of plate edges which have an adverse effect on the guiding accuracy.

• Einicke, H.: Arc welding power sources (1908-25).—A review is given of the classification, characteristics and performance data of the major power supplies produced in the German Democratic Republic.

• Dennin, G.: Strength of fillet welds produced with the CO_2-shielded welding process (1926-30). — Data obtained by analyzing the penetration and strength values of test welds were used to establish approximation formulas which make it possible to determine the increase in penetration in CO_2 welding as a function of the throat thickness of the fillet welds.

• Tassewa, S. and Höhn, W.: Welding of steels alloyed with nitrogen (1932-46). — The weldability of a number of austenitic Cr-Ni steels with high nitrogen contents was investigated and the mechanical and corrosion properties of the welds obtained with different filler metals were examined. The results are reported in tabular form.

• Hesse, G. and Ruckert, D.: Transistorized welding voltage regulator (1949-54).—In response to the demands for means to maintain constant welding parameters which are essential in automatic welding a transistorized voltage regulator ZIS 613 has been developed for the universal welding rectifier KG 400 VC/ZIS 465.

• Jaeger, F. et al.: High-frequency welding of synthetic fabrics in the garment industry (1955-62).—A general review of the current state of development and of the problems involved in the high-frequency welding of synthetic fabrics is given. Joining of thermoplastic fabrics by ultrasonic welding and other methods is predicted.

• Kudryavtsev, J. V. and Naumchenkov, N. E.: Fatigue strength of welded components for overhead cranes (1965-75).—The results of recent Russian studies of the effects of type of joint, welding process and post-weld treatment on the fatigue strength of several important crane components are reported.

• Naumann, E.: Possibilities of optimizing the layout of weld fabrication shops 1967-85).—The author describes an example where computer methods involving iteration and simulation have been used to solve the problem of optimum plant layout as applied to weld fabrication shops.

• Klasterka, F.: Four-station contour welding setup (1986-89).—The successful development of an automatic welding setup for the fabrication of the rear spring suspension of a passenger car (Model 353) is described.

• Kraus, W.: Brazing and soldering equipment-patent review (1990-96). —Patents, patent applications and design patents published in West and East Germany in 1968/69 are reviewed.

U.S.S.R.

Avtomaticheskaya Svarka 22, No. 1 (Jan. 1970).

• Seleznev, A. G. et al.: Study of the structure of the transition layer in friction welding with the aid of radioactive isotopes (21-24).—The results of a study of the structure of the contact layer in the friction welding of dissimilar metals, using tagged atoms, are reported. In the friction welding of St 30 and PI8 steels and also of St 30 and Armco iron no substantial migration of carbon atoms was observed. It is shown that there is no diffusion of carbon atoms at a depth beyond 5-10 microns.

• Krutikhovskii, V. G. and Tregubov, G. G.: Dimensions of the weld deposit as a function of the welding variables in submerged arc overlay welding with strip electrodes (25-27). —An empirical relationship was established between the width of the weld deposit and the welding parameters

(*Continued on page* 284-s)

RUDOLPH O. SEITZ is Information Specialist with Air Reduction Co., Murray Hill, N. J.